Plio-Pleistocene Ice Volume, Antarctic Climate, and the Global $\delta^{18}O$ Record

M. E. Raymo,[1]* L. E. Lisiecki,[1] Kerim H. Nisancioglu[2]

We propose that from ~3 to 1 million years ago, ice volume changes occurred in both the Northern and Southern Hemispheres, each controlled by local summer insolation. Because Earth's orbital precession is out of phase between hemispheres, 23,000-year changes in ice volume in each hemisphere cancel out in globally integrated proxies such as ocean $\delta^{18}O$ or sea level, leaving the in-phase obliquity (41,000 years) component of insolation to dominate those records. Only a modest ice mass change in Antarctica is required to effectively cancel out a much larger northern ice volume signal. At the mid-Pleistocene transition, we propose that marine-based ice sheet margins replaced terrestrial ice margins around the perimeter of East Antarctica, resulting in a shift to in-phase behavior of northern and southern ice sheets as well as the strengthening of 23,000-year cyclicity in the marine $\delta^{18}O$ record.

Although the glacial-interglacial cycles of the past 3 million years (My) represent some of the largest and most studied climate variations of the past, the physical mechanisms driving these cycles are not well understood. For the past 30 years, the prevalent theory has been that fluctuations in global ice volume are caused by variations in the amount of insolation received at critical latitudes and seasons because of variations in Earth's precession, obliquity, and eccentricity. Based mainly on climate proxy records from the past 0.5 My, but also supported by climate model results, a loose scientific consensus has emerged that variations in ice volume at precession [~23 thousand years (ky)] and obliquity (41 ky) frequencies appear to be directly forced and coherent with northern summer insolation, whereas the ~100-ky component of the ice age climate cycle results from nonlinear amplification mechanisms possibly phase-locked to summer insolation variations (*1*–*3*).

In the late Pliocene/early Pleistocene (LP/EP) interval from ~3 to 1 million years ago (Ma), however, only weak variance at 100-ky and 23-ky periods is observed in proxy ice volume records such as benthic $\delta^{18}O$. Instead, the records are dominated by 41-ky cyclicity, the primary obliquity period (Figs. 1A and 2A) (*4*–*6*) [supporting online material (SOM) text]. Given that the canonical Milankovitch model predicts that global ice volume is forced by high northern summer insolation, which at nearly all latitudes is dominated by the 23-ky precession period (Figs. 1B and 2A) (*7*), why then do we not observe a strong precession signal in LP/EP ice volume records? The lack of such a signal and the dominance of obliquity have defied understanding. Similarly, some ice modeling experiments show a dominant 41-ky periodicity, but there is always relatively more precession power in simulated ice volume than is observed in the geologic record; no ice sheet–climate model that we are aware of has been successful in reproducing the observed spectral characteristics of the LP/EP ice volume record (*8*–*10*). In every model, including our own recent ice modeling experiments that include meridional energy fluxes sensitive to varying insolation gradients (*5*, *10*), ablation is highly sensitive to summer heating and hence precession is always strongly represented in the predicted ice volume record. The strong influence of summer heating on ice sheet mass balance is also supported by more than a century of glaciological field studies [as summarized in (*11*) and shown in Fig. 3].

Here, we present a simple model of ice volume change, consistent with traditional Milankovitch theory and glaciological field studies, that predicts a sea level/$\delta^{18}O$ record that closely matches that observed from the geologic record. We used the nondimensional ice sheet–climate model of Imbrie and Imbrie (*12*), but a more sophisticated ice sheet model

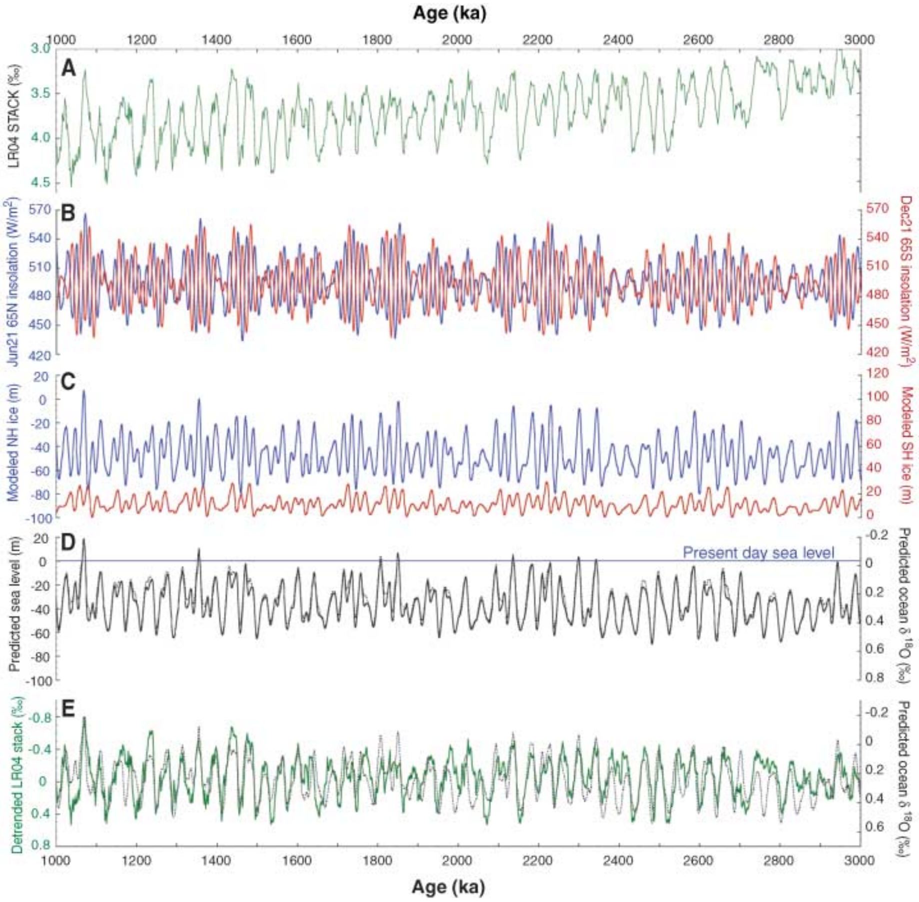

Fig. 1. Age versus (**A**) LR04 stack of >50 benthic $\delta^{18}O$ records (*6*); (**B**) 65°N summer insolation records for NH (21 June) and SH (21 December), calculated from (*7*); (**C**) NH (blue) and SH (red) modeled ice volumes, calculated as described in text; (**D**) predicted sea level (solid line) and mean ocean $\delta^{18}O$ (dashed line), derived from ice volume histories shown in (C); and (**E**) comparison of predicted mean ocean $\delta^{18}O$ and the LR04 stack detrended by a slope of 0.8‰ per My from 3 to 2.5 Ma and 0.26‰ per My from 2.5 to 1 Ma (*31*).

[1]Department of Earth Science, Boston University, 685 Commonwealth Avenue, Boston, MA 02215, USA. [2]Palaeoclimates, Bjerknes Center for Climate Research, Allegaten 55, Bergen 5007, Norway.

*To whom correspondence should be addressed. E-mail: raymo@bu.edu

would give similar results (*10*) (SOM text). Our modeled ice sheets are dominated by precession because of the assumed (and observed) dependence of ablation on summer temperatures. Our experiment differs from previous attempts to model the "41-ky world" because we allowed for a dynamic Antarctic ice sheet, as suggested by Pliocene sea level data. First, we present evidence for a more dynamic Antarctic ice sheet in the LP/EP, followed by model results and a discussion of the implications of our hypothesis.

Mid-Pliocene climate and ice sheet margins. Many marine and terrestrial studies have documented the long-term cooling that began in the early Pliocene and culminated in the growth of large Northern Hemisphere (NH) ice sheets by 2.5 Ma (*4*, *13–15*). It is also widely recognized that the mid-Pliocene before 2.9 Ma was the most recent time period consistently warmer than the present, with global temperatures elevated by as much as 3°C with respect to modern values (*16*). In particular, the interval between 3.3 and 3.0 Ma, often referred to as the "mid-Pliocene climatic optimum," is widely studied as a possible analog for a future warmer Earth (*17*).

From 3.3 to 3.0 Ma, the deep ocean $\delta^{18}O$ record is characterized by consistently more depleted isotopic values (lower than modern values by >0.5‰), indicative of warmer bottom waters and/or less global ice volume (*14–17*). Independent evidence for higher sea levels during the mid-Pliocene climate optimum comes from raised coastal terraces [35 ± 18 m relative to present (rtp) (*18*)] and Pacific atolls [up to 25 m higher rtp (*19*)]. Given that the present-day Greenland and West Antarctic ice sheet volumes are each equivalent to only 6 to 7 m of sea level (*20*), the above studies imply that a substantial volume of the present East Antarctica ice sheet (EAIS) must have melted at this time [today the EAIS is equivalent to ~54 to 55 m of sea level (*21*)]. Studies conducted on and around Antarctica suggest a warmer, partially deglaciated EAIS at this time, including extensive paleosol development (*22*), increased smectite in near-shore sediment (*23*), and less regional ice-rafted material (*24*). Recent expeditions have also found evidence for dynamic behavior of the EAIS margin throughout the Plio-Pleistocene, including less continental ice, reduced sea-ice cover, and inland penetration of warmth in the Prydz Bay region (*25*, *26*), as well as a substantial melting of the Ross ice shelf, near 1.0 Ma (*27*). Indeed, the almost completely ice-covered and poorly studied EAIS coastline (generally located between 65°S and 70°S over more than 7000 km) could have been deglaciated (melting ice sheet margin on land) for much of the late Pliocene and/or early Pleistocene, leaving little evidence today.

Ultimately, ice sheets are at the mercy of the competing forces of ablation and accumulation (Fig. 3). In East Antarctica today (Fig. 3B), virtually no melting occurs and precipitation is limited by low air temperature. Most ablation is due to calving of icebergs from ice margins at sea level (*28*) (on the West Antarctic Peninsula, by contrast, summer temperatures exceed 0°C and grass and mosses take root today). During the last glacial maximum (21 ka), Antarctica is believed to have increased in volume by 15 m of sea level equivalent (*29*), most likely by expanding onto exposed shelves as sea level fell because of NH ice sheet growth (note, in Fig. 3, that glacial cooling in and of itself would predict a decrease in mass accumulation). By comparison, Greenland today (hatched bar in Fig. 3B) experiences widespread summer melting in low altitude coastal regions that is offset by accumulation inland. During the last glacial maximum, the expanded Laurentide and Fennoscandia ice sheets would also have experienced widespread summer melting on their southern margins.

From modern glaciological observations and paleo–sea level data, we draw this conclusion: The deglaciation of a substantial fraction of the EAIS at 3 Ma, suggests that the EAIS behaved glaciologically, at that time, like a modern Greenland ice sheet. In other words, the EAIS must have overlapped the range of negative mass balance (uppermost bar in Fig. 3B). A warmer, more dynamic EAIS with a terrestrial-based melting margin, as opposed to a glaciomarine calving margin, is implied. Because such margins are strongly controlled by summer melting, Antarctic ice volume would be sensitive to orbitally driven changes in local summer insolation. When did the EAIS transition to its modern state, ringed by extensive marine ice shelves? Until now it has been assumed that it happened in concert with the well-documented NH cooling between 3 and 2.6 Ma. Here, we propose that it may not have happened until after 1 Ma.

Modeled Plio-Pleistocene ice volume history. Next, we present a forward model of global ice volume history initialized at 3 Ma with the following assumptions: (i) ice sheet mass balance is sensitive to local summer insolation; (ii) NH ice volume varies on orbital time scales between the present volume and 80 m below present sea level; and (iii) Antarctic ice volume varies between the present value and sea level that is 30 m higher than the present sea level. In other words, cool NH summers will lead to NH ice growth while, at the

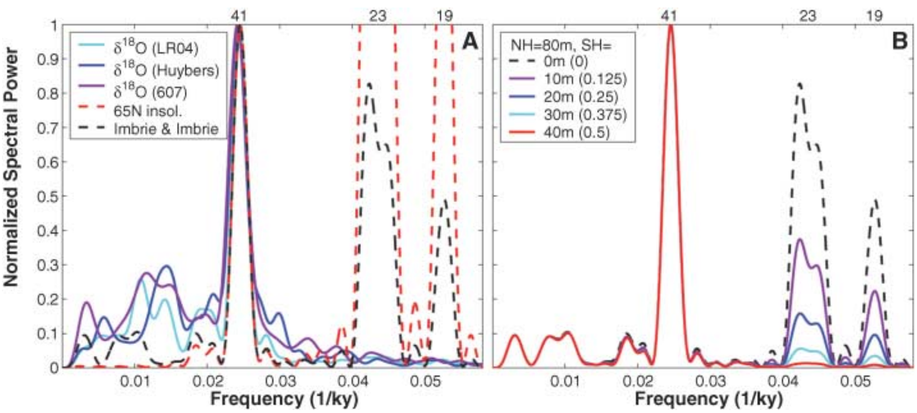

Fig. 2. (**A**) Spectra of the LR04 stack, the paleomagnetically dated $\delta^{18}O$ stack of Huybers (*57*), the paleomagnetically dated DSDP607 benthic $\delta^{18}O$ record (*4*, *34*), 21 June summer insolation at 65°N, and NH model output (Fig. 1C). All spectra are calculated over interval from 3 to 1 Ma and are normalized to each other (SOM text). (**B**) Comparison of spectra for sea level curves calculated with the use of different ratios of NH to SH ice volume change (ratio SH/NH ice given in parentheses). NH ice is always assumed to range over 80 m sea level equivalent and SH ice varies over a range of 0 to 40 m. In Fig. 1 we show the results of the 80 m/30 m experiment.

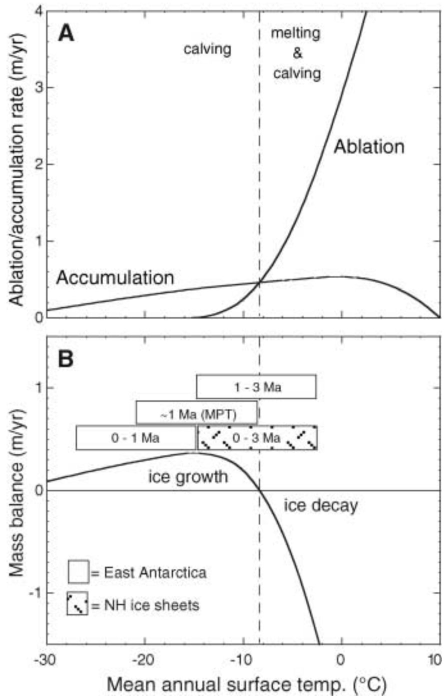

Fig. 3. Generalized dependence of ice sheet ablation rate, accumulation rate (**A**), and mass balance (**B**) on mean annual surface temperature [modified from (*58*)]. Hatched and open bars show hypothesized time evolution of NH and SH ice sheets, respectively. Vertical dashed line denotes transition from ablation-dominated to accumulation-dominated regime. MPT, mid-Pleistocene transition.

same time, warm Southern Hemisphere (SH) summers lead to ice decay in Antarctica (Fig. 1B). To predict the individual ice volume histories for each hemisphere, we used the well-known ice-climate model of Imbrie and Imbrie (*12*):

$$-dV/dt = (i + V)/\tau \qquad (1)$$

where V is ice volume, i is insolation (21 June, 65°N for NH; 21 December, 65°S for SH), and τ is a time constant which differs for ice growth and decay (see SOM text for more model details). Insolation and the modeled ice volume histories for the NH and SH (in sea level equivalents) are shown in Fig. 1, B and C. Individual ice sheet histories are dominated by both precession and obliquity frequencies (Fig. 2B), as would be expected.

Combining the two modeled ice sheet histories, one can predict global sea level (Fig. 1D). In the global ice volume/sea level signal, precession-driven responses, which are out of phase between the hemispheres, largely cancel each other out, leaving a record dominated by obliquity (Figs. 1D and 2B). Similar results would be found for any comparable ratio of northern to southern ice volume. The above assumptions about ice sheet evolution are simplistic; for instance, ice-rafted detritus (IRD) records suggest that NH ice sheets were increasing in volume over the interval from 2.9 to 2.5 Ma (*4*, *13*), whereas we assume no long-term volumetric trends in the ice sheets. If one allowed NH ice volume to gradually increase from 3 to 1 Ma, one would expect to observe a gradual increase in precession power in modeled sea level. Such an increase is observed in $\delta^{18}O$ data (SOM text and fig. S1).

One can convert modeled ice volume to $\delta^{18}O$ units by making an assumption about the mean $\delta^{18}O$ of ice at each pole (*30*). We then compared the predicted mean ocean $\delta^{18}O$ to the LR04 $\delta^{18}O$ stack (*6*) after detrending the stack for long-term global cooling (Fig. 1E). Despite some obvious mismatches in amplitude and/or structure, the overall correspondence between our model output and a global stack of more than two dozen benthic $\delta^{18}O$ records is excellent (*31*). The ability of this simple model to recreate the "41-ky world" suggests our hypothesis, the partially out-of-phase waxing and waning of ice sheets in both hemispheres over much of the Plio-Pleistocene, merits consideration. The data and model mismatches may also arise from the temperature component, time-scale errors, and geologic noise contained in the LR04 stack. Our conclusion is relatively insensitive to the sea level ranges and/or isotopic compositions assumed (sensitivity tests shown in Fig. 2B) or values chosen for the time constants in the model (SOM text). A ratio of SH to NH ice of just 13% (10 m SH/80 m NH) results in a pronounced diminishment of the precessional signal in the modeled $\delta^{18}O$/sea level record, and a ratio of 25% (20 m SH/80 m NH) results in the appearance of a "41-ky world."

Other climate proxy records. The above model reconciles the LP/EP $\delta^{18}O$ record with evidence drawn from modern glaciological studies, ice sheet–climate models, and recent ice sheet history for the strong control exerted by summer temperatures on ablation. Our hypothesis is also consistent with the presence of large ice sheets in the mid-latitudes of the United States in the LP/EP (*9*), as well as with an inferred 23-ky periodicity in melt water delivery down the Mississippi River drainage at that time (*32*). One might argue that it would require an unrealistically large warming to develop a terrestrial melting margin on the EAIS. Yet sediments recovered from an ice-covered lake in the Prydz Bay area show the presence of running water, warmer water diatoms, and mosses during the penultimate interglaciation (*33*), widely recognized as being only slightly warmer than the Holocene (*20*).

More difficult to reconcile with our proposed NH and SH ice volume histories are proxy records of sea surface temperature (SST) and IRD from the Northern and Southern Atlantic Ocean that show a strong 41-ky pacing (*4*, *13*, *24*, *34*, *35*). Indeed, the covariance of the $\delta^{18}O$, IRD, and SST records in the high latitude North Atlantic has long been invoked as sedimentological evidence that the variability observed in benthic $\delta^{18}O$ must derive in large part from the waxing and waning of ice sheets at the 41-ky periodicity in the NH (*4*, *13*, *34*). How then could large ice volume changes at the precessional period be missed? For the IRD record, we propose that the answer lies in the behavior of the two types of ice sheet margins: terrestrial and glaciomarine. On a terrestrial margin, ice sheet advance and retreat is strongly controlled by surface melt that is almost entirely dependent on summer heating. Such margins leave no imprint on marine IRD records because they are not in contact with the ocean. On the other hand, glaciomarine margins, similar to more than 90% of the Antarctic ice margin today, are the source of icebergs that deliver IRD to open ocean. Such margins are highly sensitive to sea level variations that can unpin and destabilize ice margins grounded below sea level (*28*). Indeed, both the early and late Pleistocene records of IRD in the North Atlantic show the most notable input occurring on deglaciations during which sea level is rising the fastest (*35*–*37*). In summary, calving rates on marine-based margins are controlled primarily by sea level and hence would be expected to follow the 41-ky sea level record (*38*).

The SST signal of the high-latitude Atlantic has also been shown to vary primarily at 41-ky between 1.6 and 1 Ma (*34*) (before this time, SST estimates are problematic because of no-analog/extinct species). In the late Pleistocene, Atlantic SST varies at both precession and obliquity periods; however, the obliquity rhythm dominates at latitudes of >50°N, where negligible precession is observed (*39*). At latitudes of <50°N, precession dominates with obliquity essentially disappearing south of 40°N (*39*). The controls of SST in the North Atlantic are poorly understood, although clearly late Pleistocene SST records poleward of 50°N are dominated almost exclusively by obliquity despite the known presence (from coral reef records) of 23-ky variability in ice volume (*40*). It may be that large changes in the extent of winter sea ice, possibly sensitive to mean annual or winter insolation at high latitudes (obliquity controlled), exert a more direct influence on polar and subpolar SST (*11*, *41*).

Beyond the North Atlantic region, numerous proxy records are dominated by precession, obliquity, or both frequencies in the LP/EP. None of these records rules out the existence of a precessional signal in NH or SH ice volume. African dust records (*42*) and grain-size variations in Chinese loess records (*43*) exhibit both precession and obliquity variance throughout the LP/EP. Climate-sensitive proxies from the Mediterranean region also show precession and obliquity pacing throughout the past 3 My (*44*). By contrast, tropical Pacific records (*45*, *46*) show an almost exclusive 41-ky signal in SST, although it leads $\delta^{18}O$ and hence cannot be responding to ice sheet forcing. These latter proxies are sensitive to the strength of trade winds and/or westerlies, which in turn are sensitive to meridional insolation gradients and thus obliquity (*5*, *10*, *47*).

Mid-Pleistocene transition. We know from ice core and coral reef records that late Pleistocene temperature and ice volume variations are roughly in phase between both hemispheres (*29*, *48*) and that sea level variations were paced by NH summer insolation forcing (*40*). We argue that this pattern of climate change was the inevitable consequence of long-term cooling that gradually drove the EAIS margin into the sea. We suggest that by ~1.0 Ma, high-latitude climate had cooled to the extent that it was no longer warm enough for an extensive terrestrial melting margin to exist on East Antarctica (middle bar in Fig. 3B). Ablation now occurred primarily by means of calving, and accumulation over the entire ice sheet may have resulted in the progressive thickening of the EAIS, limited only by ice stream drawdown mechanisms and moisture starvation.

Implicit in this scenario is the conclusion that sea level changes driven by NH ice sheet fluctuations became the primary control on Antarctic ice volume after ~1 Ma. When sea level dropped, the EAIS would grow out onto the continental shelf; when sea level rose, the retreat of the marine ice sheet grounding lines around Antarctica would result in rapid ice shelf disintegration. Ice volume at both poles would now vary in phase at both obliquity and precession frequencies, and $\delta^{18}O$ would thus exhibit both 23-ky and 41-ky cyclicity (as observed). These two modes of SH response (in phase versus out of phase) do not necessarily require an abrupt transition.

Conclusions. By allowing modest variations in Antarctic ice sheet size from 3 to 1 Ma, controlled by local insolation, we show that the dominant 41-ky period in marine $\delta^{18}O$ records may result from out-of-phase ice sheet growth at each pole. Individual ice volume histories in the Arctic and Antarctic realm were likely dominated by both precession (out of phase between poles) and obliquity (in phase between poles) with ice ablation strongly controlled by summer temperatures. Our hypothesis solves the conundrum of why no strong precession signal is observed in global $\delta^{18}O$ records from this time despite the well-known importance of summer temperatures on ice sheet and glacier mass balance (*49*). Our hypothesis also predicts the presence of a dynamic EAIS in the LP/EP characterized by a terrestrial ablation margin at latitudes between 65°S and 70°S. We also predict that the record of local temperature recorded by deuterium isotopes in ice cores (should ice this old ever be recovered) would be in phase with SH insolation at the precession frequency. In the NH, sites sensitive to the southern margin of the NH ice sheet should show a record of variability much like that depicted in Fig. 1C.

We further propose that long-term cooling resulted in a transition from a primarily land-based to primarily marine-based EAIS margin about 1.0 Ma, resulting in the mid-Pleistocene transition and the strengthening of 23-ky cycles in the $\delta^{18}O$ record. Ice sheet volume may have increased at both poles at this time because of the establishment of positive globally synchronous feedbacks (such as albedo and CO_2) at the precession frequency (*50*). Lastly, the strengthening of CO_2 and albedo feedbacks by enhanced sea level fall or aridity, in conjunction with long-term global cooling, may have led to the establishment of NH ice sheets large enough to survive summer insolation maxima of low intensity, a necessary prerequisite for the development of the ''100-ky'' cycle (*51*).

References and Notes

1. J. Imbrie *et al.*, *Paleoceanography* **7**, 701 (1992).
2. D. Paillard, *Rev. Geophys.* **39**, 325 (2001).
3. E. Tziperman, M. E. Raymo, P. Huybers, C. Wunsch, *Paleoceanography*, in press.
4. M. E. Raymo, W. F. Ruddiman, J. Backman, B. M. Clement, D. G. Martinson, *Paleoceanography* **4**, 413 (1989).
5. M. E. Raymo, K. Nisancioglu, *Paleoceanography* **18**, 10.1029/2002PA000791 (2003).
6. L. E. Lisiecki, M. E. Raymo, *Paleoceanography* **20**, 10.1029/2004PA001071 (2005).
7. J. Laskar, F. Joutel, F. Boudin, *Astron. Astrophys.* **270**, 522 (1993).
8. A. Berger, X. S. Li, M. F. Loutre, *Quat. Sci. Rev.* **18**, 1 (1999).
9. P. U. Clark, D. Pollard, *Paleoceanography* **13**, 1 (1998).
10. K. H. Nisancioglu, Ph.D. thesis, Massachusetts Institute of Technology, Cambridge, MA (2004); available online (http://hdl.handle.net/1721.1/16703).
11. G. H. Denton, R. B. Alley, G. Comer, W. S. Broecker, *Quat. Sci. Rev.* **24**, 1159 (2005).
12. J. Imbrie, J. Z. Imbrie, *Science* **207**, 943 (1980).
13. N. J. Shackleton *et al.*, *Nature* **307**, 620 (1984).
14. M. E. Raymo, *Annu. Rev. Earth Planet. Sci.* **22**, 353 (1994).
15. M. Mudelsee, M. E. Raymo, *Paleoceanography* **20**, 10.1029/2005PA001153 (2005).
16. A. C. Ravelo, D. H. Andreasen, M. Lyle, A. O. Lyle, M. W. Wara, *Nature* **429**, 263 (2004).
17. H. J. Dowsett *et al.*, *Global Planet. Change* **9**, 169 (1994).
18. H. J. Dowsett, T. M. Cronin, *Geology* **18**, 435 (1990).
19. B. R. Wardlaw, T. M. Quinn, *Quat. Sci. Rev.* **10**, 247 (1991).
20. K. M. Cuffey, S. J. Marshall, *Nature* **404**, 591 (2000).
21. P. Huybrechts, D. Steinhage, F. Wilhelms, J. L. Bamber, *Ann. Glaciol.* **30**, 52 (2000).
22. G. J. Retallack, E. S. Krull, J. G. Bockheim, *J. Geol. Soc. London* **158**, 925 (2001).
23. J. Junttila, K. Strand, *Eos Trans. AGU* **86**, Fall Meet. Suppl., abstract PP41B-0639 (2005).
24. L. Murphy, D. A. Warnke, C. Andersson, J. Channell, J. Stoner, *Paleoceanography* **182**, 183 (2002).
25. P. G. Quilty, *Eos Trans. AGU* **86**, Fall Meet. Suppl., abstract PP51F-04 (2005).
26. A. K. Cooper, P. E. O'Brien, in *Proc. Ocean Drill. Prog. Sci.*, A. K. Cooper, P. F. O'Brian, C. Richter, Eds. (2004), vol. 188, ch. 1; available online (http://www-odp.tamu.edu/publication/188_SR/synth/synth.htm).
27. R. P. Scherer, *Eos Trans. AGU* **86**, Fall Meet. Suppl., abstract PP43C-05 (2005).
28. D. I. Benn, D. J. A. Evans, *Glaciers and Glaciation* (Arnold Press, London, 1998).
29. S. E. Bassett, G. Milne, J. X. Mitrovica, P. U. Clark, *Science* **309**, 925 (2005).
30. Assuming NH ice averages –30 per mil (‰) and SH ice averages –45‰ results in a predicted ocean $\delta^{18}O$ amplitude that is a little more than half of that observed (implying deep ocean temperature changes of a few degrees; Fig. 1, D and E). The difference in NH and SH ice sheet isotopic composition also results in a slight decrease of the precessional component of the modeled curve (dashed line in Fig. 1D). If NH glacial ice is assumed to be more depleted, –40‰ for example, then the modeled $\delta^{18}O$ approaches the amplitude of the LR04 stack (Fig. 1A), implying that much of LP/EP signal is due to ice volume change. Ultimately, ongoing development of independent temperature proxies may allow us to isolate the ice volume component in ocean $\delta^{18}O$ records and provide a better modeling target.
31. The overall correlation coefficient between stack and modeled $\delta^{18}O$ from 2.7 to 1.2 Ma is 0.68. Small age model adjustments to the stack, within the range of age model uncertainty (<5 ky), can increase the correlation to 0.75. Both correlation values decrease slightly (to 0.63 and 0.72, respectively) when the full interval of 3 to 1 Ma is used. The stack is detrended by a slope of 0.8‰ per My from 3 to 2.5 Ma and 0.26‰ per My from 2.5 to 1 Ma.
32. J. E. Joyce, L. Tjalsma, J. Prutzman, *Geology* **21**, 483 (1993).
33. D. A. Hodgson *et al.*, *Quat. Sci. Rev.* **25**, 179 (2006).
34. W. F. Ruddiman, M. E. Raymo, D. G. Martinson, B. M. Clement, J. Backman, *Paleoceanography* **4**, 353 (1989).
35. K. A. Venz, D. A. Hodell, C. Stanton, D. A. Warnke, *Paleoceanography* **14**, 42 (1999).
36. M. E. Raymo, K. Ganley, S. Carter, D. W. Oppo, J. McManus, *Nature* **392**, 699 (1998).
37. J. F. McManus, D. W. Oppo, J. L. Cullen, *Science* **283**, 971 (1999).
38. High-resolution studies (*36*, *37*) also reveal that episodes of less notable IRD input occur on millennial time scales (Dansgaard-Oeschger/Heinrich events), events that are believed to reflect solar or stochastically forced instability in the marine ice margin grounded in Hudson Bay [reviewed in (*52*)]. It may be that successive increments of sea level fall, obliquity-paced in our hypothesis, require the marine-based components of ice sheets to constantly readjust their grounding lines seaward. Millennial-scale interruptions in the delivery of IRD to the open ocean may occur when an ice margin is growing out to a new stable grounding line. When a new grounding line is established, the renewed calving of icebergs would occur, contributing to regional cooling and freshening of ocean surface waters and thus promoting the development of sea ice cover and weakening thermohaline convection. In other words, one need not invoke any millennial-scale forcing but only the slow relentless drive of orbital-scale changes in sea level.
39. W. F. Ruddiman, A. McIntyre, *Geol. Soc. Am. Bull.* **95**, 381 (1984).
40. W. G. Thompson, S. L. Goldstein, *Quat. Sci. Rev.,* in press.
41. M. E. Raymo, D. Rind, W. F. Ruddiman, *Paleoceanography* **5**, 367 (1990).
42. P. B. deMenocal, *Science* **270**, 53 (1995).
43. Y. Sun, S. C. Clemens, Z. An, Z. Yu, *Quat. Sci. Rev.* **25**, 33 (2006).
44. L. J. Lourens, F. J. Hilgen, J. Gudjonsson, W. J. Zachariasse, *Mar. Micropaleontol.* **19**, 49 (1992).
45. Z. Liu, T. D. Herbert, *Nature* **427**, 720 (2004).
46. M. Medina-Elizalde, D. W. Lea, *Science* **310**, 1009 (2005).
47. S.-Y. Lee, C. J. Poulsen, *Paleoceanography* **20**, 10.1029/2005PA001161 (2005).
48. T. Blunier, E. J. Brook, *Science* **291**, 109 (2001).
49. By contrast, in a late Oligocene/early Miocene benthic $\delta^{18}O$ record (*53*), both precession and obliquity variance are observed. This result is consistent with the presence of ice sheets in only one hemisphere (Antarctica) at that time.
50. In the late Pleistocene, ice core CO_2 records are strongly paced by obliquity and more weakly influenced by precession (*54*). Given the uncertainties in the controls of atmospheric CO_2, our hypothesis cannot predict how the early Pleistocene CO_2 record will vary. For instance, if CO_2 variations are controlled by sea level (*55*), then the development of in-phase polar climate behavior at the mid-Pleistocene transition would cause global CO_2 variations to occur at the precession period for the first time. If high-latitude aridity and dust supply control CO_2 (*56*), then the possible dominance of one hemisphere over the other (due to greater land mass for instance) could impart a precession signal to the early Pleistocene CO_2 record. In this case, we might still expect the precession signal in the CO_2 record to get stronger at the mid-Pleistocene transition if high-latitude aridity, as well as ice volume, began to vary in phase. Lastly, if positive climate feedbacks act preferentially on obliquity time scales (*54*), then the ice volume signal at the 41-ky period could be additionally amplified relative to precession.
51. M. E. Raymo, *Paleoceanography* **12**, 577 (1997).
52. G. C. Bond *et al.*, in *Geophys. Monogr. Am. Geophys. Union 112* (American Geophysical Union, Washington, DC, 1999), pp. 35–58.
53. J. C. Zachos, N. J. Shackleton, J. S. Revenaugh, H. Pälike, B. P. Flower, *Science* **292**, 274 (2001).
54. W. F. Ruddiman, *Quat. Sci. Rev.* **22**, 1597 (2003).
55. J. C. Latimer, G. M. Filippelli, *Paleoceanography* **16**, 627 (2001).
56. R. B. Alley, E. J. Brook, S. Anandakrishnan, *Quat. Sci. Rev.* **21**, 431 (2002).
57. P. Huybers, *Quat. Sci. Rev.*, in press.
58. P. Huybrechts, in *Climate of the 21st Century: Changes and Risks*, J. Lozan, H. Grabl, P. Hupfer, Eds. (GEO Wissenschaftliche Auswertungen, Hamburg, 2001), pp. 221–226.

59. We thank K. Lawrence, J. Fastook, D. Marchant, B. Ruddiman, P. Huybrechts, J. Kennett, B. Curry, R. Scherer, D. Bowen, P. Huybers, and D. Oppo for assisting us on this project, either by reading the manuscript or providing helpful guidance and information; E. Tziperman for ongoing discussions of Milankovitch and climate; and four anonymous reviewers whose comments greatly improved the manuscript. M.E.R. acknowledges the support of NSF grant ATM-0220681. L.E.L. is supported by a NOAA Climate and Global Change postdoctoral fellowship.

Supporting Online Material

www.sciencemag.org/cgi/content/full/1123296/DC1
SOM Text
Figs. S1 to S4
Tables S1 to S3
References

1 December 2005; accepted 9 June 2006
Published online 22 June 2006;
10.1126/science.1123296
Include this information when citing this paper.